AIP | Journal of Applied Physics

Site-controlled Ag nanocrystals grown by molecular beam epitaxy—Towards plasmonic integration technology

Adam Urbańczyk and Richard Nötzel

Citation: J. Appl. Phys. **112**, 124302 (2012); doi: 10.1063/1.4768914
View online: http://dx.doi.org/10.1063/1.4768914
View Table of Contents: http://jap.aip.org/resource/1/JAPIAU/v112/i12
Published by the American Institute of Physics.

Related Articles

Surface-enhanced Raman scattering (SERS) based on copper vanadate nanoribbon substrate: A direct bio-detection without surface functionalization
J. Appl. Phys. 112, 114309 (2012)

Intrinsic localized modes in two-dimensional vibrations of crystalline pillars and their application for sensing
J. Appl. Phys. 112, 104326 (2012)

Influence of Cr2O3 nanoparticles on the physical properties of polyvinyl alcohol
J. Appl. Phys. 112, 093525 (2012)

Nano-environment effects on the luminescence properties of Eu3+-doped nanocrystalline SnO2 thin films
J. Chem. Phys. 137, 184704 (2012)

Reactive-ion-etched graphene nanoribbons on a hexagonal boron nitride substrate
Appl. Phys. Lett. 101, 203103 (2012)

Additional information on J. Appl. Phys.

Journal Homepage: http://jap.aip.org/
Journal Information: http://jap.aip.org/about/about_the_journal
Top downloads: http://jap.aip.org/features/most_downloaded
Information for Authors: http://jap.aip.org/authors

ADVERTISEMENT

JOURNAL OF APPLIED PHYSICS **112**, 124302 (2012)

Site-controlled Ag nanocrystals grown by molecular beam epitaxy—Towards plasmonic integration technology

Adam Urbańczyk[1,a)] and Richard Nötzel[2]
[1]*COBRA Research Institute on Communication Technology, Department of Applied Physics, Eindhoven University of Technology, 5600 MB Eindhoven, The Netherlands*
[2]*Institute for Systems based on Optoelectronics and Microtechnology (ISOM), ETSI Telecommunication, Technical University of Madrid, Ciudad Universitaria s/n, 28040 Madrid, Spain*

(Received 1 June 2012; accepted 10 November 2012; published online 17 December 2012)

We demonstrate site-controlled growth of epitaxial Ag nanocrystals on patterned GaAs substrates by molecular beam epitaxy with high degree of long-range uniformity. The alignment is based on lithographically defined holes in which position controlled InAs quantum dots are grown. The Ag nanocrystals self-align preferentially on top of the InAs quantum dots. No such ordering is observed in the absence of InAs quantum dots, proving that the ordering is strain-driven. The presented technique facilitates the placement of active plasmonic nanostructures at arbitrarily defined positions enabling their integration into complex devices and plasmonic circuits. © *2012 American Institute of Physics*. [http://dx.doi.org/10.1063/1.4768914]

I. INTRODUCTION

Plasmonics is a rapidly developing branch of science concerned with manipulating light at nanometer length scales utilizing metallic nanostructures which support propagating surface plasmons and localized surface plasmon resonances (LSPRs). It already provided significant contributions in fields such as biosensing[1,2] or energy conversion.[3] Recently, there is an increasing interest in active plasmonics,[4–7] where one combines such metallic nanostructures with active media in order to obtain new functionalities including the generation of light through spasing,[5,8] loss-compensated surface plasmon propagation,[9] and ultrafast all-optical switching[7,10] or amplification.[11] Those active elements are of nanoscale dimensions and if they were integrated into one device or plasmonic circuit they could offer performance comparable or superior to integrated electronics[12] and provide additional functionalities.[13] This, however, requires highly reproducible fabrication of individual metallic nanostructures with high quality in order to control their optical properties,[14] precise positioning of the metal with respect to the active structures with single nanometer precision necessary for optimum coupling,[15] as well as arbitrary positioning on large length scales in order to enable integration of different plasmonic structures. We have recently demonstrated that it is possible to grow, by molecular beam epitaxy (MBE), epitaxial metal nanocrystals (NCs) of In[16] and Ag[17] that support LSPRs in the near-infrared wavelength region. Such NCs self-align on top of optically active near-surface In(Ga)As quantum dots (QDs) due to strain driven ad-atom migration. This self-assembly phenomenon offers a route to synthesize individual active plasmonic nanostructures with the required precision. Self-assembly has, however, one drawback, it cannot allow for arbitrary placement of structures on the substrate. It facilitates long-range ordering only in relatively simple periodic arrangements and with high spatial frequencies.[18] That is why it is necessary to consider hybrid approaches utilizing both bottom-up, as well as top-down methods like it is done in the case of deterministic positioning of QDs.[19]

Here, we propose to use guided self-assembly of epitaxial Ag NCs on lithographically defined structures. We demonstrate that the Ag NCs grow preferentially on near surface QDs that are placed in etched holes. This allows for simultaneous precise QD-Ag NC coupling by controlling the QD capping layer thickness and long-range ordering of such hybrid structures with large NC separations and very good yield. After the coupled QD-Ag structures are synthesized at the desired positions, they can be planarized by a thin dielectric layer for additional deposition of a metal film for further processing. This would allow to define passive plasmonic waveguides connecting the active structures, thus enabling truly integrated active plasmonic circuitry. This concept is shown schematically in Figure 1.

II. EXPERIMENTAL DETAILS

All investigated samples were grown using a custom solid source MBE system with an attached metal deposition chamber on undoped, singular (100) oriented GaAs wafers. The substrate patterns were obtained by optical lithography and wet chemical etching in 40:1 citric acid:hydrogen peroxide, where the citric acid was a 50% aqueous solution of the corresponding monohydrate. The patterns consisted of arrays of holes with 10 μm pitch, diameters of 1.5 and 2.5 μm, and etched to a depth of 70 nm. After processing, the patterned substrates were cleaned by stripping the photoresist in acetone, O_2 plasma treatment, 10 min dip in concentrated H_2SO_4 and final rinsing with copious amounts of deionized water. The growth procedure begun with thermal oxide removal at 580 °C. Afterwards a 100-nm-GaAs buffer layer was deposited at 520 °C. In order to obtain a better surface morphology, the III/V ratio was adjusted during the GaAs growth so that a (2×4) surface reconstruction was

a)Author to whom correspondence should be addressed. Electronic mail: adam.jan.urbanczyk@gmail.com.

 © 2012 American Institute of Physics

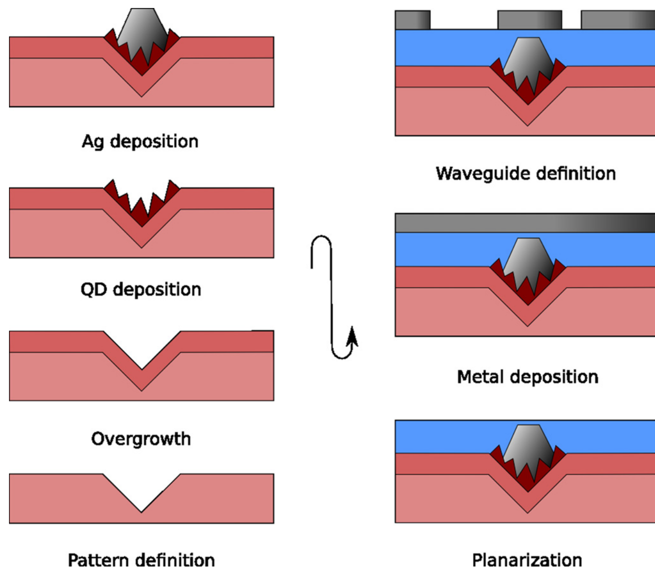

FIG. 1. Proposed process for integrating active plasmonic nanostructures obtained by strain-driven self-alignment of Ag NCs on top of site-controlled QDs.

observed. Then 1.6 monolayer (ML) of InAs was deposited with a growth rate of 0.002 ML/s. This resulted in QD formation only inside the etched holes. The QDs were capped with 6 nm AlAs, maintaining the rather symmetric QD shapes and a high aspect ratio compared to thin GaAs capping due to the smaller surface migration length of Al compared to that of Ga.[20] Now the samples were cooled down and transferred to the Ag deposition chamber. Approximately 0.1 nm Ag was deposited with a growth rate of 0.005 nm/min and at a substrate temperature of 350–400 °C. Such low growth rate and high temperature were chosen to obtain a low nucleation density, preventing excess Ag NCs between the lithographically defined holes. Finally, the samples were cooled down and taken out of the MBE system. In both chambers reflection high-energy electron diffraction (RHEED) was used to monitor the growth process. The surface morphology of the obtained samples was characterized using tapping-mode atomic force microscopy (AFM) under ambient conditions.

III. RESULTS AND DISCUSSION

Figure 2 presents the RHEED patterns observed in different azimuths after the deposition of Ag on a planar substrate under the conditions reported previously.[17] The appearance of sharp diffraction spots, i.e. bulk transmission diffraction patterns marked by the red circles, is evidence for the epitaxial growth of the Ag NCs on (100) GaAs. It is deduced from the diffraction patterns taken in the different azimuths that the epitaxial relation is $(100)_{Ag} \parallel (100)_{GaAs}$ and $[001]_{Ag} \parallel [001]_{GaAs}$ in accordance with the data from the literature.[21] Under optimum conditions for site-controlled growth of Ag NCs no diffraction spots due to the NCs can be observed, as their density is too low. The identical morphology and orientation, however, allow to infer that under such conditions they have the same epitaxial relation. In all cases, after the deposition of Ag, the streaky RHEED pattern of the reconstructed GaAs surface remains clearly visible. This excludes the possibility of reaction of deposited metal with the underlying substrate and alloy formation.

The results of the AFM measurements for patterned substrates with the large, 2.5-μm-diameter holes with and without the presence of InAs QDs are presented in Figures 3 and 4, respectively. Clearly, in the case of the patterned substrates with QDs shown in the overview AFM image in Figure 3(a), all the Ag NCs position on the sidewalls of the holes, where the QDs nucleated. This is most evident in the AFM image at enlarged magnification of a single hole, shown in Figure 3(b) where the InAs QDs and Ag NCs, indicated by arrows, are both clearly visible. The InAs QDs are the dense and shallow, round or elliptical, lens-shaped structures, while the Ag NCs are the much higher pyramidal-shaped structures with rectangular base. This assignment is evident from the previous experiments[17] comparing the surface morphology with or without the growth of InAs QDs or Ag NCs, respectively.

Due to the relatively high InAs deposition temperature and sub-critical (on planar substrates) coverage the InAs QDs grow only on the sidewalls of the etched holes; there are no QDs at the flat bottom of these large holes. Moreover, there is a clear preference for nucleation on the {11-1}B-like facets, identified from the orientation and slope in AFM line scans. The Ag NCs follow the QDs, independent of the varying size and shape of the QDs on the hole sidewalls. Ag NCs are found neither in the planar areas between the holes nor at the flat bottom of the holes.

In the case of the patterned substrate without deposited InAs QDs, no ordering of the Ag NCs is found. The Ag NCs nucleate randomly without any recognition of the pattern, as clearly depicted in the overview AFM image in Figure 4(a) and the AFM image at enlarged magnification of a single hole in Figure 4(b).

The significant roughness of the sidewalls does not facilitate preferential nucleation of the Ag NCs. In the whole

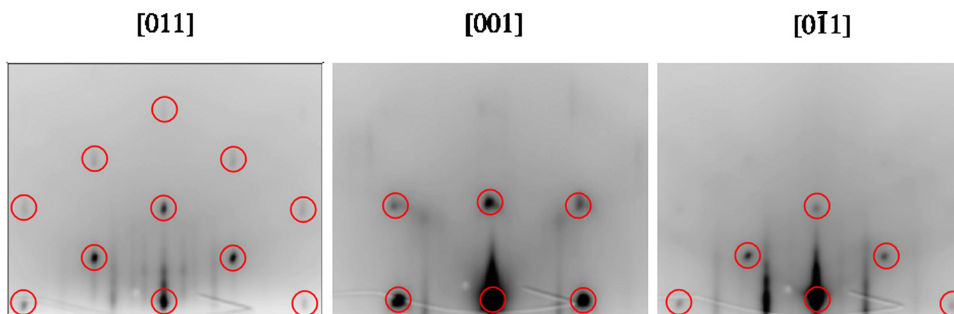

FIG. 2. RHEED patterns observed along [011], [001], and [0-11] after the deposition of Ag on GaAs (100). The circles mark the diffraction spots of the Ag NCs.

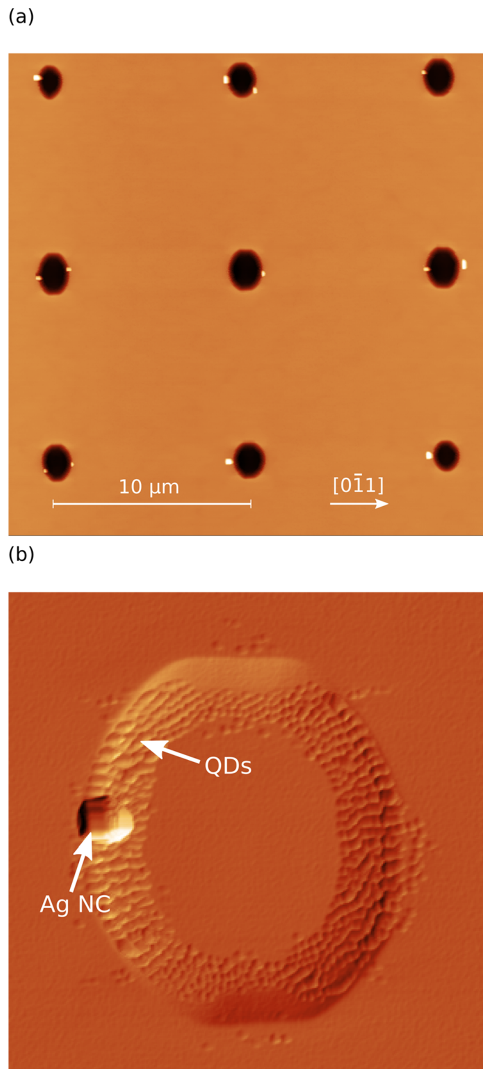

FIG. 3. (a). AFM measurements image of Ag NCs (white rectangles) on hole-patterned GaAs substrates with InAs QDs underneath. The patterned hole diameter is 2.5 μm. The scan field is 25 by 25 μm^2. (b) AFM image at enlarged magnification of a single hole. The image is artificially shaded to make the InAs QDs with the Ag NC on top clearly visible. Arrows indicate the InAs QDs and Ag NC for clarity.

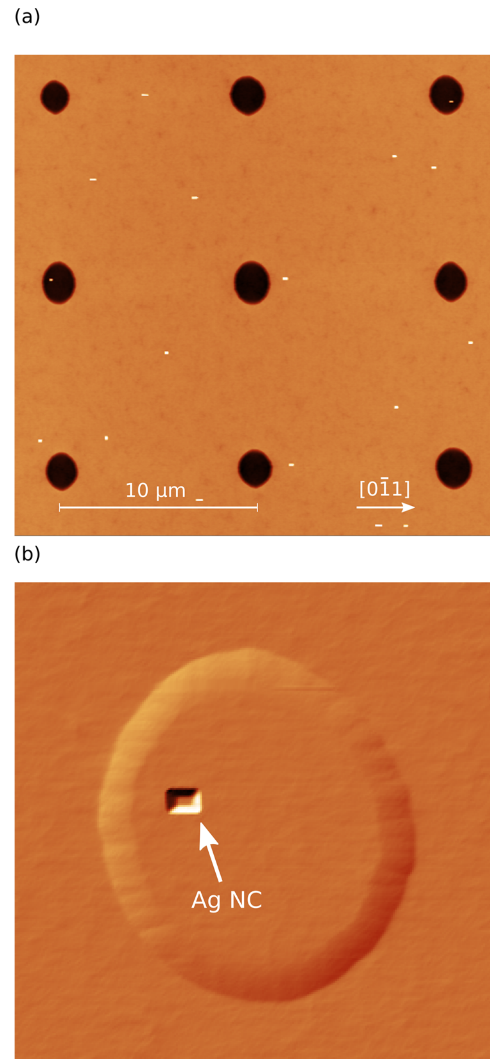

FIG. 4. AFM images of Ag NCs (white rectangles) on hole-patterned GaAs substrates without InAs QDs underneath. The patterned hole diameter is 2.5 μm. The scan field is 25 by 25 μm^2. (b) AFM image at enlarged magnification of a single hole. The image is artificially shaded as in Figure 3(b) to make the Ag NC clearly visible. The arrow indicates the Ag NC for clarity.

measurement area there are no Ag NCs positioned on the sidewalls. This fact is consistent with the low relative area of sidewalls compared to the flat surface accounting for low probability of nucleation at such sites. This clearly demonstrates that the surface morphology is not the driving force behind the observed ordering, unlike in the case of the InAs QDs. Hence, we conclude that the Ag NC ordering is strain-driven—the NCs can accommodate the lattice mismatch more easily on sites with near-surface InAs QDs due to the larger lattice constant of InAs as compared to GaAs or AlAs.

To be more precise, the following mechanisms are discussed in the literature for the position controlled epitaxial growth of nanostructures: preferential nucleation at step edges, selectivity of growth on different facets on non-planar patterned substrates, selective area growth on substrates patterned with dielectric masks, and directional adatom migration on strain-modulated templates. The first three mechanisms are excluded from the experimental findings and setup. Hence, the positioning of the Ag NCs is attributed to strain-driven adatom migration towards locations where the lattice mismatch and, therefore, strain energy are minimized and this, again, is on top of the InAs QDs with the locally larger lattice constant. This is similar to the mechanism discussed for the explanation of the well-known strain-correlated stacking of QDs.[22]

The size of the Ag NCs and QDs differs since the final size of the Ag NCs is controlled by their growth conditions and not by the nucleation process. Hence, nucleation and growth need to be clearly distinguished. The nucleation process due to strain driven adatom migration defines the position of the Ag NCs on top of the QDs and their growth, depending on substrate temperature and deposition amount defines their final size, as is the case of unpatterned substrates.

Despite the bottom-up nature of the ordering process, it is surprisingly reproducible. On a $25 \times 25\ \mu m^2$ area no Ag NCs are found on the flat surface between the holes, which constitutes the majority of the scanned area. Interestingly,

AFM measurements (data not shown) performed on unprocessed areas of the same sample reveal a much lower NC density and larger NC size than those on the patterned areas, 0.008 NCs per μm^2 and an average height of 120 nm versus 0.02 NCs per μm^2 with an average height of 50 nm, respectively. This demonstrates that patterned substrates, in addition to position control, allow to control the size and density of the metal NCs. This is important for obtaining the desired LSPR wavelength. According to our previous studies of the optical properties of Ag NCs on GaAs, the NCs of the size obtained in the holes support LSPR in the desired near-infrared wavelength range coinciding with the QD emission wavelength.[17]

Due to the relatively large area of the hole sidewalls as compared to the average base size of the Ag NCs, the demonstrated positional accuracy of the ordering has a significant random component. This issue can be solved by decreasing the hole size, thus decreasing the sidewall area available for preferential nucleation of the Ag NCs. For an initial hole diameter of 1.5 μm the AFM measurement results are presented in Figure 4(a). After GaAs buffer overgrowth, the initially round holes change into oblate-shaped ones. This is due to the anisotropic ad-atom surface migration during growth of GaAs which has a higher rate in the [0-11] direction.[23] This causes faster closing of the holes in this direction, ultimately resulting in the disappearance of the planar areas inside the holes. Only the sidewalls remain allowing for much more precise positioning of the Ag NCs. Additionally, the statistical analysis of the nucleation sites reveals that the NCs prefer the long axis of symmetry of the holes in 60% of the cases. This further increases the placement accuracy, as well as opens up the possibility of rational design of the pattern shape in order to achieve complex structures like NC dimers, shown in the inset of Figure 5(a).

In order to demonstrate the feasibility of truly nanoscale positioning accuracy, it is necessary to overcome the resolution limitations of the used lithographic process. This is achieved by intentionally underexposing the pattern. In case of the 2.5-μm-diameter hole pattern this results in arrays of two adjacent submicron holes. After overgrowth, the holes have average sizes of 600 by 400 nm^2 and the already discussed asymmetric shape. The achieved positional accuracy is better than this value because the Ag NCs nucleate preferentially on the symmetry axis of the holes along the [011] direction. As seen in Figure 5(b), in this way, it is also possible to obtain paired Ag NCs with submicron separation. Furthermore, it shows that it is possible to grow one Ag NC in each hole, provided the hole size is sufficiently small and that in this case all NCs are in a similar position, in the center of the hole with basically identical size and shape.

Ultimately, in order to achieve sub-10-nm positioning accuracy, it is obviously necessary to scale down the hole size even further with simultaneous reduction of the QD number in the holes. This can be done by using, for example, high-resolution optical, electron beam or nanoimprint lithography. An additional important issue is the control of the hole morphology. It might be beneficial in further studies to use an As_2 instead of As_4 flux in order to prevent the anisotropic deformation of the holes during GaAs overgrowth allowing for fine tuning of the hole size by changing the buffer layer thickness.

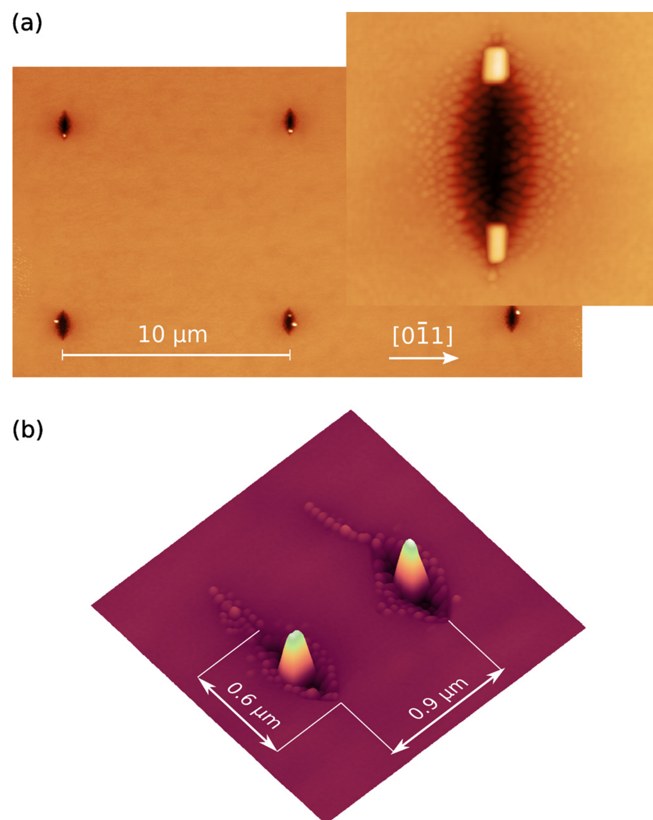

FIG. 5. AFM measurements of Ag NCs on hole-patterned GaAs substrates with InAs QDs underneath. The patterned hole diameter in (a) is 1.5 μm. Under exposure in case of the 2.5 μm diameter holes in (b) results in arrays of submicron hole pairs. The scan field in (a) is 25 by 13 μm^2.

IV. CONCLUSIONS

To conclude, we have demonstrated site-controlled growth of Ag NCs using lithographic patterning and strain-driven preferential nucleation on top of near surface InAs QDs. With reducing size of the patterned holes submicron precise positioning was achieved together with single nanometer precise control of the near surface InAs QD to Ag NC distance. This allows for both long-range ordering of the NCs, as well as optimizing the Ag-QD plasmonic coupling. Clearly, our concept of epitaxial self-alignment on patterned substrates is feasible for the realization of ordered and reproducible arrays of active plasmonic nanostructure hybrids paving the way for the integration of active and passive plasmonic nanostructures enabling complex LSPR-based devices and plasmonic circuits.

ACKNOWLEDGMENTS

The authors thank F. W. M. van Otten, T. de Vries, and E. Smalbrugge for help with the sample preparation.

[1]J. Homola, Chem. Rev. **108**, 462 (2008).
[2]K. M. Mayer and J. H. Hafner, Chem. Rev. **111**, 3828 (2011).
[3]H. A. Atwater and A. Polman, Nat. Mater. **9**, 205 (2010).

[4]M. I. Stockman, J. Opt. **12**, 024004 (2010).
[5]M. A. Noginov, G. Zhu, A. M. Belgrave, R. Bakker, V. M. Shalaev, E. E. Narimanov, S. Stout, E. Herz, T. Suteewong, and U. Wiesner, Nature **460**, 1110 (2009).
[6]A. Boltasseva and H. A. Atwater, Science **331**, 290 (2011).
[7]M. Abb, P. Albella, J. Aizpurua, and O. L. Muskens, Nano Lett. **11**, 2457 (2011).
[8]R. F. Oulton, V. J. Sorger, T. Zentgraf, R. Ma, C. Gladden, L. Dai, G. Bartal, and X. Zhang, Nature **461**, 629 (2009).
[9]J. Grandidier, G. C. des Francs, S. Massenot, A. Bouhelier, L. Markey, J. Weeber, C. Finot, and A. Dereux, Nano Lett. **9**, 2935 (2009).
[10]N. Large, M. Abb, J. Aizpurua, and O. L. Muskens, Nano Lett. **10**, 1741 (2010).
[11]M. A. Noginov, G. Zhu, M. Mayy, B. A. Ritzo, N. Noginova, and V. A. Podolskiy, Phys. Rev. Lett. **101**, 226806 (2008).
[12]R. Zia, J. A. Schuller, A. Chandran, and M. L. Brongersma, Mater. Today **9**, 20 (2006).
[13]Z. Jacob and V. M. Shalaev, Science **334**, 463 (2011).
[14]P. Biagioni, J. Huang, and B. Hecht, Rep. Prog. Phys. **75**, 024402 (2012).
[15]P. Anger, P. Bharadwaj, and L. Novotny, Phys. Rev. Lett. **96**, 113002 (2006).
[16]A. Urbańczyk, G. J. Hamhuis, and R. Nötzel, Appl. Phys. Lett. **96**, 113101 (2010).
[17]A. Urbańczyk, F. W. M. van Otten, and R. Nötzel, Appl. Phys. Lett. **98**, 243110 (2011).
[18]T. Mano, R. Nötzel, G. J. Hamhuis, T. J. Eijkemans, and J. H. Wolter, J. Appl. Phys. **95**, 109 (2004).
[19]P. Atkinson, M. B. Ward, S. P. Bremner, D. Anderson, T. Farrow, G. A. C. Jones, A. J. Shields, and D. A. Ritchie, Jpn. J. Appl. Phys., Part 1 **45**, 2519 (2006).
[20]F. Ferdos, S. Wang, Y. Wei, M. Sadeghi, Q. Zhao, and A. Larsson, J. Cryst. Growth **251**, 145 (2003).
[21]J. Massies and N. T. Linh, J. Cryst. Growth **56**, 25 (1982).
[22]Q. Xie, A. Madhukar, P. Chen, and N. Kobayashi, Phys. Rev. Lett. **75**, 2542 (1995).
[23]K. Ohta, T. Kojima, and T. Nakagawa, J. Cryst. Growth **95**, 71 (1989).